AMBIENT VIBRATIONS OF AGE-OLD MASONRY TOWERS: RESULTS OF LONG-TERM DYNAMIC MONITORING IN THE HISTORIC CENTRE OF LUCCA.

Riccardo M. Azzara[1], Maria Girardi[2], Valerio Iafolla[3,4], David M. Lucchesi[3,2], Cristina Padovani[2], Daniele Pellegrini[2]

[1] Istituto Nazionale di Geofisica e Vulcanologia (INGV), Osservatorio Sismologico di Arezzo, Italy
[2] Institute of Information Science and Technologies "A. Faedo" ISTI-CNR, Pisa, Italy
[3] National Institute for Astrophysics, INAF-IAPS, Rome, Italy
[4] Assist in Gravitation and Instrumentation, AGI srl, Rome, Italy.

This is an Accepted Manuscript of an article published by Taylor & Francis in [International Journal of Architectural Heritage] on [12 December 2019], available online:
[https://doi.org/10.1080/15583058.2019.1695155].

Abstract

The paper presents the results of an ambient vibration monitoring campaign conducted on so-called "Clock Tower" (Torre delle Ore), one of the best known and most visited monuments in the historic centre of Lucca.

The vibrations of the tower were continuously monitored from November 2017 to March 2018 using high-sensitivity instrumentation. In particular, four seismic stations provided by the Istituto Nazionale di Geofisica e Vulcanologia and two three-axial accelerometers developed by AGI S.r.l., spin-off of the Istituto Nazionale di Astrofisica, were installed on the tower. The measured vibration level was generally very low, since the structure lies in the middle of a limited traffic area. Nevertheless, the availability of two different types of highly sensitive and accurate instruments allowed the authors to follow the dynamic behaviour of the tower during the entire monitoring period and has moreover provided cross-validation of the results.

1 Introduction

The first attempts to use ambient vibrations to characterize the dynamic properties of buildings date back to the 1970's (Trifunac 1970). Nowadays, this technique has become standard practice (Celebi

2017, Gallipoli et al. 2010, Kaya and Safak 2015, Peeters et al. 1999, Prieto et al. 2010) thanks to the availability of sensitive instrumentation for measurement of low-amplitude vibrations, together with powerful algorithms and hardware for large dataset analysis. Ambient vibration monitoring is in fact very convenient, provided that sufficiently long records are available (Brincker 2015), since it allows avoiding artificial vibration sources such as vibrodynes, thereby facilitating experiment management. Moreover, long-term ambient vibration measurements furnish important information on the sources of vibration, the influence of the environmental parameters on the structural dynamic properties and finally on the structural health status. Indeed, changes over time in a building's dynamic properties, such as modal properties (Doebling et al. 1996) or wave velocities (Todorovska 2009), represent effective damage indicators, provided that the natural changes due to seasonal and daily environmental effects are taken into account. Long-term monitoring plays an important role when a structure is subjected to high vibration levels, such as those induced by traffic or construction sites (Wyjadlowski 2017), or when the structure is located in high-seismicity areas (Celebi 2017, Todorovska 2009, Trifunac 1970). More recently, the study of the dynamic effects on buildings of the surrounding environment has became a challenging research topic, involving disparate expertise from the fields of physics, geology and engineering, and sometimes referred to as "urban seismology" (Diaz et al. 2017), (Green et al. 2016), (Ritter et al. 2005). Moreover, the recent availability of low-cost measurement devices has encouraged the testing of large accelerometer networks for monitoring purposes (Barsocchi et al. 2018), (D'Alessandro et al. 2018), (Clementi et al. 2018), including through participative approaches as in (Matarazzo et al. 2018), where citizens were directly involved in monitoring the vibrations of bridges with their own smartphones (which are normally equipped with MEMS devices to measure accelerations).

With regard to the world's architectural heritage and monuments, the first examples of dynamic monitoring through ambient vibrations for damage detection purposes date back to (Gentile and Saisi 2007), and (Ramos et al. 2010). A great deal of effort has been made to study the effects of

56 traffic on ancient monuments, noteworthy amongst which is the work of (Pau and Vestroni 2008)
57 and (Bongiovanni et al. 2017) on dynamic characterization of the Colosseum, (Roselli et al. 2017)
58 on other monuments in Rome, (Chiostrini et al. 1995), (Lacanna et al. 2016) and (Lacanna et al.
59 2019) in the historic centre of Florence, (Azzara et al. 2017) on the Maddalena Bridge in Borgo a
60 Mozzano, and (Erkal 2017) on the traffic-induced vibrations on a minaret in Turkey. The
61 availability of large datasets yielded by continuous monitoring of historic structures is however
62 relatively recent. Some examples can be found in (Baraccani et al. 2017) on the Asinelli tower in
63 Bologna, (Masciotta et al. 2017) on the Saint Torcato church, (Ubertini et al. 2017) on the ambient
64 vibrations of the San Pietro bell tower in Perugia, (Lorenzoni et al. 2018) on post-earthquake
65 vibration checks of some monumental buildings in l'Aquila, (Cabboi et al. 2017) on the continuous
66 vibration monitoring of an age-old tower in Northern Italy, (Azzara et al. 2018a) on the San
67 Frediano bell tower in the historic centre of Lucca, and (Kita et al. 2019) on the Consoli Palace in
68 Gubbio.
69 The present paper is aimed at investigating the dynamic behaviour of a medieval tower located in a
70 historic centre and subjected to vibrations from the surrounding environment, the main goals being:
71 to characterize the main sources of vibration, the trend of the tower's dynamic properties over time,
72 and the tower's response to the activities in the historic centre. To this end, the authors rely on a
73 dataset obtained from five months of continuous measurements (November 2017 to March 2018) on
74 the so-called "Torre delle Ore" (henceforth Clock Tower) in the historic centre of Lucca. The
75 measurements were recorded via two different sets of high-sensitivity instruments, both installed on
76 the tower during the monitoring period: four three-axial seismometric stations (each equipped with
77 a SL06 24-bit digitizer coupled to a SS20 electrodynamic velocity transducer) developed by SARA
78 Electronic Instruments S.r.l. and furnished by the Istituto Nazionale di Geofisica e Vulcanologia
79 (INGV), and two accelerometers designed for applications in the fields of gravitation, space
80 dynamics and oceanographic research (Iafolla et al. 2015), and specifically adjusted for the current
81 experiment by Assist in Gravitation and Instrumentation (AGI S.r.l.) of Rome, a spin-off enterprise

of the Istituto Nazionale di Astrofisica (INAF). The combined use of the two different kinds of measurement devices has allowed for a comparison of the instruments' performance, as well as cross-validation of the results obtained for the Clock Tower, which have also been corroborated by the outcomes of two-year continuous monitoring conducted on the nearby San Frediano bell tower (Azzara et al. 2018a, 2018b).

In addition, exploitation of the different characteristics of the seismometers and accelerometers has made it possible both to explore the dynamic behaviour of the tower and to highlight the effects of environmental vibrations in a wide frequency range. To the best of the authors' knowledge, the issues addressed in this paper are far from being fully investigated and the reported results constitute a novel contribution to understanding the dynamic response of the architectural heritage to anthropic and natural vibration sources.

2 The experimental campaign on the Clock Tower

Lucca was renowned in the past for the large number of towers in its skyline: of more than one hundred during Middle Ages, only ten or so of these fascinating monuments have survived until today (Figure 1). The Clock Tower is one of the best known and most visited age-old towers in Lucca, thanks to the peculiar shape of its bell chamber, which is clearly visible and recognizable throughout the entire historic centre. Built by local families (Concioni 1988), since the last decade of the 15th century the Clock Tower has been used as a civic building, taking its name from the big clock visible on its southern facade (Figure 2). The Clock Tower rises at the corner between the roads named Via Arancio and Via Fillungo, one of the most popular in Lucca's historic centre; the adjacent buildings abut the tower on two sides for a height of about 13 m and constitute asymmetric boundary conditions for the tower's structure. The Clock Tower is 48.4 m high at the top of the bell chamber; it has a rectangular cross section of about 5.1 x 7.1 m and walls of thickness varying from about 1.77 m at the base to 0.85 m at the top. Two barrel vaults are set inside the tower at heights of about 12.5 and 42.3 m. The bell chamber, made up of four masonry pillars connected by elliptical

arches, stands on the upper barrel vault and is covered by a pavilion roof constructed of wooden trusses and rafters. With regard to the materials constituting the masonry tower, visual inspection reveals that the masonry from the base up to a height of 15 m is made up of regular stone blocks and thin mortar joints. The upper walls are instead composed of regular stone blocks and bricks, also with thin joints. The pillars of the bell chamber are made of brick masonry.

On 25 November 2016, during a preliminary experimental campaign, the response of the Clock Tower to ambient vibrations was monitored for a few hours via four SARA SS20 three-axial seismometric stations. The instruments were moved along the tower's height by adopting three different layouts and combining data in order to identify four natural vibration frequencies and mode shapes of the tower, as described in (Pellegrini et al. 2017). Data collected in this experiment also allowed evaluating the mechanical properties of the tower's constituent materials via model updating procedures, as described in (Girardi et al. 2019). Table 1 summarizes the frequencies calculated in the preliminary campaign of November 2016 (Pellegrini et al. 2017). The mode shapes of the tower corresponding to the first four frequencies determined by taking advantage of the different layouts used for mapping the tower' vibrations, are shown in Figure 3. The first two frequencies refer to bending modes along the *x* (first) and *y* (second) directions, while the third is a torsional mode and the fourth is a torsional-bending mode involving movements of the structure's upper parts. Since the tower is located in the historic centre, in a limited traffic area, the environmental vibrations are quite low and do not allow to estimate frequencies and mode shapes higher than the fourth.

In November 2017 a continuous long-term ambient vibration monitoring experiment was begun with the fitting of six instruments along the tower's height: four SARA SS20 seismometric stations (tri-axial velocimeters, Fig. 4, SARA Electronic Instruments, https://www.sara.pg.it) owned by the INGV, named in the following S.942, S.943, S.944, S.945, and two tri-axial accelerometers (Fig. 5) provided by the firm Assist in Gravitation and Instrumentation (AGI S.r.l.), named in the following

134 S.1 and S.2. The INGV sensors were coupled with a 24-bit digitizer and the signal was sampled at
135 100 Hz. The AGI data were acquired by a laptop at a sampling frequency of 20 Hz using a 24-bit
136 digitizer. This sampling frequency corresponds to a Nyquist frequency of 10 Hz and then to a very
137 narrow band; nevertheless the frequency range is sufficient enough to catch the main natural
138 frequencies of the tower calculated in (Pellegrini et al. 2017) and recalled in Table 1.
139 With regard to the main characteristics of the instruments used in the monitoring campaign, the
140 SS20 velocity transducers have a nominal sensitivity of 200 V/(m/s), eigenfrequency of 2 Hz, and
141 usable band from 0.1 to 100 Hz (the signal has to be suitable corrected via the transfer function of
142 the system). The AGI accelerometers have an acceleration noise density of $2 \cdot 10^{-8}$ g/$\sqrt{\text{Hz}}$,
143 sensitivity in the order of 200 V/g, and usable band from 10^{-5} to 50 Hz. It is worth noting that
144 together the instruments can cover a very wide band of frequencies.
145 The instrumentation was kept running on the tower up to March 2018. Figure 6 shows the layout of
146 the sensors along the tower during the experiment: seismic station S.942 was placed at the base,
147 collecting data from the ground, S.943 was at the height of 24 m above street level, the remaining
148 two stations S.943 and S.944 were placed on the bell chamber, at about +42 m above street level.
149 The AGI stations were both installed in the upper part of the structure, S.2 at +37 m and S.1 on the
150 bell chamber level.
151 Safety reasons suggested not taking measurements during the opening period of the tower, which
152 attracts many visitors during spring and summer and whose interior is very narrow with a poor
153 place for the installation of instruments and cables. Thus, the experiment was carried out in winter
154 to take advantage of the tower being closed to the public. Nevertheless, the experimental campaign
155 encountered several problems, due to adverse weather conditions, a number of electrical blackouts,
156 and the presence of many people working inside the tower and disrupting the data acquisition. In
157 particular, the INGV seismic stations and the AGI sensor S.1 were removed on 8 December 2017
158 after an electrical shutdown. The velocimeters were installed again on 11 January 2018, while the
159 AGI accelerometers were fitted to the tower on 11 February 2018. Moreover, from 29 January to 11

February 2018 all instrumentation was removed to allow a public ceremony to be held inside the tower. On 17 November 2017 a fifth INGV seismic station was installed inside a private flat in a building adjacent to the tower, and left active for some hours, with the aim of recording the natural frequencies of the building and evaluating its influence on the tower's dynamic behaviour. The data collected during the experiments (about 970 hours of recordings for the SS20 seismic stations and 1110 hours for the AGI instrumentations) are stored in a database hosted by the Mechanics of Materials and Structures Lab of ISTI-CNR in Pisa.

3 Data analysis and results

3.1 Dynamic identification and behaviour over time

All data have been analysed via the Covariance-driven Stochastic Subspace Identification method (SSI/Cov), an Operational Modal Analysis (OMA) technique in the time-domain implemented in the MACEC code (Reynders et al. 2016). To this end, the data have been divided into one-hour long datasets. Moreover, the data recorded by the INGV stations have also been processed via Experimental Modal Analysis (EMA), by applying the Complex Mode Indicator Function (CMIF) method (Shih et al., 1988) implemented in TruDI (Pellegrini 2019) and considering the seismic station at the base (S942) as input signal. These last analyses were needed to take into account the composition of the signals at the base of the tower, whose spectrum shows a clear energy accumulation at about 3 Hz in the *x*-direction, along Via Fillungo. This same frequency was also recorded in the same direction by the station installed in the flat adjacent to the tower. In the authors' opinion, it represents a natural frequency of the building next to the tower and does not belong to the tower structure itself. Such conclusion is confirmed by the CMIF analysis, shown in Figure 7, where the three eigenvalues of the matrix $H[j\omega]^H H[j\omega]$ are reported vs. frequency, with $H[j\omega]$ the Frequency Response Function matrix of the system, estimated by the H_1 estimator, (Maia and Silva, 1997) and ω the circular frequency. Figure 7 refers to the analysis of a one-hour long

185 dataset recorded by the INGV seismic stations: the four peaks represent the identified four
186 frequencies of the tower, the 3 Hz frequency being much less accentuated.
187 The tower's frequencies are reported in Table 2, where the mean values (evaluated over the entire
188 monitoring period from November 2017 to March 2018) of the four frequencies are reported,
189 together with their relative differences (evaluated on the 1st and 99th percentile) for the two different
190 instruments. The frequencies values measured on the Clock Tower are in good agreement with
191 those of other towers with similar geometries (Bartoli et al. 2017). The frequency values vs. time
192 are reported in Figures 8 and 9 for the SS20 and the AGI instruments, respectively. The mean
193 values evaluated by the two instruments are in very good agreement. The first and the second
194 frequencies were detected by the two instruments in all records, and the variation in the two
195 frequencies is on the order of 3%. This variation is also in good agreement with the findings of
196 another long-term dynamic monitoring conducted on the San Frediano bell tower in Lucca (Azzara
197 et al. 2018a). The third frequency was also detected by the seismic stations in almost all records,
198 while the fourth frequency only appears when the excitation level in the tower's structure was
199 increased (it was detected in about the 30% of the records), and its values appear to be widely
200 dispersed. A fifth frequency at about 5.7 Hz was also detected in about 30% of the records. With
201 regard to the modal damping ratios, reported in Table 3, they are widely dispersed with variations
202 on the order of hundreds of percentage points. Their values vary from 4% for the highest frequency,
203 to 0.5% for the first. The values yielded by the seismic stations are generally higher than those from
204 the accelerometers.
205
206 Figures 10 and 11 show further comparisons of the results obtained via the two instruments. In
207 particular, Figure 10 shows the trend of the tower's fundamental frequency from 7 to 8 December
208 2017, extracted from the AGI (blue) and the SS20 (red) devices. The very good agreement between
209 the two measurements indicates that the fluctuations exhibited in the frequency values do not
210 depend on the instruments' functioning, but are rather due to environmental factors. Figure 11

211 shows a comparison of the hourly maximum accelerations (absolute values) recorded by the
212 instruments during that same period. It is worth noting that maxima in the acceleration values
213 correspond to minima in the frequency values. In fact, a look at the weather those days revealed
214 very bad conditions, with strong wind velocities (see also Figure 15), thereby suggesting a
215 connection between the frequency reduction shown in Figure 10 and the action of the wind, which
216 due to the masonry's inability to withstand large tensile stresses, tends to decrease the tower's
217 stiffness (see also Figure 16).
218
219 ***3.2 Effects of environmental factors***
220 With regard to the influence of temperature on the tower's dynamic behaviour, Figure 12 shows the
221 correlation of the first two natural frequencies with air temperature, measured by a sensor located in
222 the Lucca Botanical Gardens, in Lucca's historic centre. The figure confirms the findings of other
223 long-term vibration monitoring campaigns on historical towers (Cabboi et al. 2017), (Ubertini et al.
224 2017), including that carried out on the San Frediano bell tower in Lucca (Azzara et al. 2018a):
225 frequencies tend to increase with temperature. This behaviour is confirmed from a numerical point
226 of view, by the results described in (Girardi et al. 2017), which reports on a nonlinear FE analysis of
227 the Clock Tower conducted by modelling the effects of the thermal variations on the structure's
228 frequencies. The numerical simulation supports the hypothesis that an increase in temperature
229 induces a reduction in the fracture strains inside masonry, thus increasing the global stiffness of the
230 structure.
231 With regard to negative temperature values, Figure 12 reveals opposite trend for frequencies, which
232 turn out to increase when the temperature decreases. This phenomenon was mainly observed in the
233 latter part of February 2018, when temperatures persistently decreased below zero, as highlighted
234 by Figure 13. Correspondingly, the figure shows the change in the frequency trend. The behaviour
235 below freezing has also been reported for similar weather conditions in (Ubertini et al. 2017) and
236 (Cabboi et al. 2017), where the increasing of frequencies when temperature goes below zero is

237 ascribed to the fact that ice tends to close micro-cracks and then stiffen the masonry. It is also worth
238 noting that, as long as the temperature remains above zero, frequencies respond to temperature
239 variations with a phase shift in time, most likely connected to the thermal inertia of the tower,
240 while, below zero, the frequency and temperature appear to be in phase.
241 The trend over time of the maximum accelerations recorded by AGI sensors, after high-pass
242 filtering of the signals (with cutoff frequency of 0.1 Hz), is shown in Figure 14. The vibration level
243 in the tower is very low, generally under $2 \cdot 10^{-3}$ m/s^2, thanks to restrictions to vehicular traffic in
244 force in the Lucca historic centre. The figure highlights an increase in the tower's vibration level
245 during the Christmas holiday period (from 22 December to 1 January), connected to the increased
246 pedestrian traffic in the historic centre, with a peak on New Year's Day. The figure also reveals a
247 systematic increase in the accelerations, on average of one order of magnitude, from 9 February
248 onward. This is due to the ringing of the tower bells, which had been suspended for restoration of
249 the ancient clock and was restarted on 16 January 2018. The bell system is composed of three
250 bronze bells, fixed at their supports and rung by hammers each quarter an hour in the *x* direction
251 (along Via Fillungo). Indeed, Figure 14 shows significant amplification along *x* (blue dots).
252 With regard to the environmental parameters that could influence the acceleration levels on the
253 tower, Figure 15 plots the daily average values of the maximum hourly accelerations in the *x* (blue)
254 and *y* (red) directions, for about a month, together with the daily maximum wind speed recorded at
255 Pieve di Compito, about 10 km from the Lucca historic centre (data available at
256 www.sir.toscana.it). The figure clearly shows a correspondence between the peaks in the
257 acceleration levels and those in the wind speed.

258 Figure 16 reports the correlation between the maximum acceleration experimented by the tower and
259 its natural frequencies and shows that frequencies tend to decrease as the amplitude of acceleration
260 increases. This trend is not unexpected and can be attributed to masonry inability to withstand

tensile stresses. Similar results for masonry-like materials are obtained via analytical models in (Girardi and Lucchesi 2010).

3.3 Sources of vibration

Figures 17 and 18 provide information on the tower' vibrations over time in the band [0, 25] Hz. In particular, Figure 17 shows the spectrogram of the signal recorded by S.942, at the base of the tower, in the period 18 November to 26 November 2017, for the three channels *x* (up), *y* and *z* (bottom). The tower's natural frequencies are clearly visible in the band [0, 10] Hz (horizontal lines), as well as the 3 Hz frequency of the building adjacent to the tower, along the *x* direction. As a result of anthropogenic activity, the power frequency increases in the entire band during the daytime, in particular during week-ends (18-19 November, 25-26 November). The three-dimensional spectrogram of channel *x* plotted in Figure 18 also highlights other anthropogenic activity between 20 and 25 Hz, which could be attributed to traffic in the historic centre. At about 12:30 (UTC) on 19 November, there is a clear frequency peak, which can be attributed to the M4.4 Parma earthquake reported in Table 4.

Many seismic events have been detected on the tower during the monitoring period. Table 4 shows the main earthquakes recorded, while Table 5 reports the teleseismic events identified in the signals. Figure 19 shows the teleseismic record of the Peru earthquake, which occurred at 09:18.44 (UTC) with a magnitude of 7.1, and was recorded at about 09:33 (UTC) by the instruments on the tower. In particular, the figure shows the signals recorded by the SS20 seismic stations at different levels along the tower's height in the *x* direction. The same event was also recorded by the S.2 accelerometer. At such a considerable distance from the epicentre, the seismic signal loses its high frequency content and becomes recognizable only at low frequencies. The records in the Figure were obtained by filtering the signals via a Butterworth band-pass filter with lower cut-off frequency of 0.04 Hz and a higher cut-off cut at 1 Hz. It is worth noting that after the first arrival of the waves the event remains clearly recognizable in the signals for long time.

Analyzing the low frequency content of the recorded signals can provide further information on movements of the tower. Figure 20 shows the signals recorded by the S.2 accelerometer from 11 to 14 January 2018 along the *x* (up) and *y* (bottom) directions. The signals in the figure were low-pass filtered with a cut-off frequency of 0.5 Hz, and clearly reveal a slow oscillation with period of about 24 hours. The same oscillations can be detected in the temperature signal (Figure 21) measured by the sensor inside the instrument. The temperature signal is however not in phase with the accelerations, thus demonstrating that the oscillations of the accelerometric signal are not a direct effect of temperature on the instrument. It is also worth noting that the signals along the *x* (North-South direction) and *y* (East-West direction) directions present a phase shift of 3 to 6 hours, and the *y* signal is delayed with respect to that along *x*. A possible interpretation of these oscillations lies in the daily temperature variations caused by exposure of the tower to the sun. As the exposure of the façades changes during the day, the tower appears to twist as shown in the figures. A measure of the displacements induced by this effect at the top of the tower can be easily obtained from the figures. In fact, for small oscillations, the modulus of the horizontal acceleration expressed in *g* coincides with the inclination angle of the tower in radians. Thus, taking into account the actual position of the instrument (at +37 m), horizontal displacements turn out to be on the order of 3-4 mm for both directions. These low-frequency displacements seem to be the main components of the total horizontal displacements experienced by the tower in normal conditions (i.e. in the absence of earthquakes or other strong dynamic actions). In any case, this data should be complemented by further measurements at the ground and static measurements as well.

4 Conclusions

The paper presents the results of an ambient vibration monitoring campaign conducted using high-sensitivity instrumentation on the Lucca Clock Tower from November 2017 to March 2018. In particular, four seismic stations provided by the INGV and two three-axial accelerometers

311 developed by AGI S.r.l were installed on the tower. The combined use of two different kinds of
312 measurement devices allowed for a comparison of the instruments' performance, as well as cross-
313 validation of the results obtained for the Clock Tower. In addition, exploiting the different
314 characteristics of seismometers and accelerometers made it possible both to explore the dynamic
315 behaviour of the tower and highlight the effects of environmental vibrations over a wide range of
316 frequency.
317 Analysis of the large dataset collected on the tower has yielded the following main results:
318 a) despite the low vibration levels, the main sources of vibration have been identified, as have
319 the dynamic characteristics of the tower;
320 b) the chief factors influencing the tower's dynamic properties are: temperature, wind speed,
321 ringing bells, crowd movements, traffic around the historic centre, and micro-tremors;
322 c) the instruments on the tower are able to clearly detect both earthquakes at epicentral distance
323 of up to hundreds of kilometres and, in the low frequency range, teleseismic sequences;
324 d) day-to-day movements of the tower can be also deduced by analysing the low-frequency
325 signals;
326 e) the simultaneous presence of the two instruments on the tower provides a detailed cross-
327 validation of the results.
328 This study shows the potentials of continuous long-term monitoring in both investigating the
329 influence of the surrounding environment on heritage structures and providing important
330 information, such as the variation of dynamic properties over time and sources of vibration, which
331 can be used to assess their structural health.
332 **Acknowledgements**

333 This research has been partially supported by the Fondazione Cassa di Risparmio di Lucca
334 (TITANIO project, 2016-2018) and the Region of Tuscany and MIUR (MOSCARDO project,
335 FAR-FAS 2014, 2016–2018). These supports are gratefully acknowledged.

References

1. Azzara, R.M., G. De Roeck, M. Girardi, C. Padovani, D. Pellegrini, and E. Reynders. 2018a. The influence of environmental parameters on the dynamic of the San Frediano bell tower in Lucca, *Engineering Structures* 156: 175-187.
2. Azzara, R.M., M. Girardi, C. Padovani, and D. Pellegrini. 2018b. Experimental and numerical investigations on the seismic behaviour of the San Frediano bell tower in Lucca, *Annals of Geophysics*, 61, doi: 10.4401/ag-8025.
3. Azzara, R.M., A. De Falco, M. Girardi, and D. Pellegrini. 2017. Ambient vibration recording on the Maddalena Bridge in Borgo a Mozzano (Italy): data analysis, *Annals of Geophysics*, 60, 4, 2017, S0441, doi: 10.4401/ag-7159.
4. Baraccani, S., M. Palermo, R.M. Azzara, G. Gasparini, S. Silvestri, and T. Trombetti. 2017. Structural interpretation of data from static and dynamic structural health monitoring of monumental buildings, *Key Engineering Materials*, 747, 431-439.
5. Barsocchi, P., P. Cassarà, F. Mavilia, and D. Pellegrini. 2018. Sensing a city's state of health: Structural Monitoring System by Internet-of-Things wireless sensing devices, *IEEE Consumers Electronics Magazine,* 7(2), 8287063, 22-31.
6. Bartoli, G., M. Betti, A.M. Marra, and S. Monchetti. 2017. Semiempirical formulations for estimating the main frequency of slender masonry towers. *Journal of Performance of Constructed Facilities,* 31 (4): 04017025.
7. Bongiovanni, G., G. Buffarini, P. Clemente, D. Rinaldis, and D. Saetta. 2017. Dynamic characteristics of the Amphitheatrum Flavium northern wall from traffic-induced vibrations, *Annals of Geophysics*, 60, 4, S0439, doi: 10.4401/ag-7178.

8. Brincker, R., and C. Ventura. 2015. *Introduction to Operational Modal analysis,* Wiley.
9. Cabboi, A., C. Gentile, and A. Saisi. 2017. From continuous vibration monitoring to FEM-based damage assessment: Application on a stone-masonry tower. *Construction and Building Materials,* 156:252–265.
10. Celebi, M., T. Kashima, S.F. Ghaharic, S. Koyama, and E. Taciroğlu. 2017. Before and after retrofit behavior and performance of a 55-story tall building inferred from distant earthquake and ambient vibration data. *Earthquake Spectra.*33(4):1599-1626.
11. Chiostrini, S., F. Lancieri, A. Marradi, M. Nocentini, and A. Vignoli. 1995. Numerical evaluation and experimental measurements of traffic-induced vibrations, Transactions on Modelling and Simulation vol 10, WIT Press, ISSN 1743-355X.
12. Clementi, F., A. Pierdicca, G. Milani, V. Gazzani, M. Poiani, and S. Lenci. 2018. Numerical model upgrading of ancient bell towers monitored with a wired sensors network. 10th International Masonry Conference, IMC 2018 (No. 222279, pp. 2308-2318). International Masonry Society.
13. Concioni, G. 1988. La Torre delle Ore fra tradizione e realtà storica. Rivista di Archeologia, Storia, Costume [Sezione delle Seimiglia dell'Istituto Storico Lucchese], Year XVI, No. 4 (October-December, 1988):3-28.
14. D'Alessandro, A. , G. Vitale, S. Scudero, R. D'Anna, G. Passafiume, L. Greco, S. Speciale, D. Patanè, O, Torrisi, S. Di Prima, S. Magiagli, and G. Tusa. 2018. Real-time urban seismic network and structural monitoring by means of accelerometric sensors: Application to the historic buildings of Catania (Italy). *IEEE International Conference on environmental Engineering EE2108. Proceedings.* p. 1-5.
15. Díaz, J., M. Ruiz , P.S. Sánchez-Pastor, and P. Romero. 2017. Urban Seismology: on the origin of earth vibrations within a city, *www.nature.com/scientificreports*, DOI:10.1038/s41598-017-15499-y.

16. Doebling, S.W., C.R. Farrar, M.B. Prime, and D. Shevitz. 1996. Damage Identification and Health Monitoring of Structural and Mechanical Systems from Changes in their Vibration Characteristics: A Literature Review. No. LA-13070-MS. Los Alamos National Lab., NM (United States).
17. Erkal, A. 2017. Transmission of Traffic-induced Vibrations on and around the Minaret of Little Hagia Sophia. *International Journal of Architectural Heritage*, 11(3):349–362.
18. Gallipoli, M.R., M. Mucciarelli, B. Šket-Motnikar, P. Zupančić, A. Gosar, S. Prevolnik , M. Herak, J. Stipčević, D. Herak, Z. Milutinović, and T. Olumćeva. 2010. Empirical estimates of dynamic parameters on a large set of European buildings. *Bulletin of Earthquake Engineering*. 8:593–607 DOI 10.1007/s10518-009-9133-6.
19. Gentile, C., and A. Saisi. 2007. Ambient vibration testing of historic masonry towers for structural identification and damage assessment. *Construction and Building Materials*, 21(6):1311-1321.
20. Girardi, M., and M. Lucchesi. 2010. Free flexural vibrations of masonry beam-columns. Journal of Mechanics of Materials and Structures, 5(1):143-159.
21. Girardi, M., C. Padovani, and D. Pellegrini. 2017. Effects of the stress field on the dynamic properties of masonry bell towers. *AIMETA 2017 - Proceedings of the 23rd Conference of the Italian Association of Theoretical and Applied Mechanics,* 3, 216-229.
22. Girardi, M., C. Padovani, D. Pellegrini, and L. Robol. 2019. A model updating procedure to enhance structural analysis in the FE code NOSA-ITACA. *Journal of Performance of Constructed Facilities*, 33(4):04019041.
23. Green, D.N., I.D. Bastow, B. Dashwood, and S.E.J. Nippress. 2016. Characterizing Broadband Seismic Noise in Central London. *Seismological Research Letters*, 88 (1): 113-124.
24. Iafolla, L., E. Fiorenza, V. A. Iafolla, C. Carmisciano, L. Montani, M. Burlando, P. De Gaetano, and G. Solari. 2015. OS-IS a new method for the sea waves monitoring,

412 MTS/IEEE OCEANS 2015. Discovering Sustainable Ocean Energy for a New World.
413 Genova, 17 September 2015, Article number 7271432.
414 25. Kaya, Y., and E. Safak. 2015. Real-time analysis and interpretation of continuous data from
415 structural health monitoring (SHM) systems. *Bullettin of Earthquake Engineering.* 13:917–
416 934.
417 26. Kita, A., N. Cavalagli, and F. Ubertini. 2019. Temperature effects on static and dynamic
418 behavior of Consoli Palace in Gubbio, Italy. *Mechanical Systems and Signal Processing*,
419 120:180-202.
420 27. Lacanna, G. , M. Ripepe, E. Marchetti, M. Coli, and C.A. Garzonio. 2016. Dynamic
421 response of the Baptistery of San Giovanni in Florence, Italy, based on ambient vibration
422 test. *Journal of . Cultural Heritage*, 20:632–640.
423 28. Lacanna, G., M. Ripepe, M. Coli, R. Genco, and E. Marchetti. 2019. Full structural dynamic
424 response from ambient vibration of Giotto's bell tower in Firenze (Italy), using modal
425 analysis and seismic interferometry. *NDT and E International,* 102:9–15.
426 29. Lorenzoni, F., M. Caldon, F. da Porto, C. Modena, and T. Aoki. 2018. Post-earthquake
427 controls and damage detection through structural health monitoring: applications in
428 l'Aquila. *Journal of Civil Structural health Monitoring.* 8(2):217-236.
429 30. Maia, N.M.M., and J.M.M. Silva. 1997. Theoretical and Experimental Modal Analysis.
430 Research Studies Press Ltd.
431 31. Masciotta, M.G., L.F. Ramos, and P.B. Lourenço. 2017. The importance of structural
432 monitoring as a diagnosis and control tool in the restoration process of heritage structures: A
433 case study in Portugal. *Journal of . Cultural Heritage*, 27:36–47.
434 32. Matarazzo, T.J., P. Santi, S. N. Pakzad, K. Carter, C. Ratti, B. Moaveni, C. Osgood, and N.
435 Jacob. Crowdsensing Framework for Monitoring Bridge Vibrations Using Moving
436 Smartphones. 2018. *Proceedings of the IEEE.* 106 (4):577-593.

437 33. Pau, A., and F. Vestroni. 2008. Vibration analysis and dynamic characterization of the
438 Colosseum, *Structural Control and Health Monitoring*. 15:1105–1121, DOI:
439 10.1002/stc.253.
440 34. Peeters, B., and G. De Roeck. 1999. Reference-based stochastic subspace identification for
441 output-only modal analysis, Mech Syst Signal Process;13(6):855–78.
442 35. Pellegrini, D. 2019. TruDI software - Version 2.0 - A MATLAB code for structural dynamic
443 identification, Technical Report ISTI-CNR.
444 36. Pellegrini, D., M. Girardi., C. Padovani, and R.M. Azzara. 2017. A new numerical
445 procedure for assessing the dynamic behaviour of ancient masonry towers. Papadrakakis M.
446 and Fragiadakis M. (eds), COMPDYN 2017, 6th International Conference on
447 Computational Methods in Structural Dynamics and Earthquake Engineering, Proceedings.
448 37. Prieto, G.A., J.F. Lawrence, A.I. Chung, and M.D. Kohler. 2010. Impulse Response of Civil
449 Structures from Ambient Noise Analysis, *Bullettin of Seismological Society of America*,
450 100, 5A, 2322–2328, doi: 10.1785/0120090285.
451 38. Ramos, L.F., L. Marques, P.B. Lourenco, G. De Roeck, and A. Campos-Costa. 2010.
452 Monitoring historic masonry structures with operational modal analysis: two case studies,
453 *Mechanical Systems and Signal Processing*. 24:1291–1305.
454 39. Reynders, E., K. Maes, G. Lombaert, and G. De Roeck. 2016. Uncertainty quantification in
455 operational modal analysis with stochastic subspace identification: Validation and
456 applications. *Mech. Syst. Signal Process,* 66-67:13-30.
457 40. Ritter, J.R.R., S.F. Balan, K.P. Bonjer, T. Diehl, T. Forbriger, G. Mărmureanu, F. Wenzel,
458 and W. Wirth. 2005. Broadband urban seismology in the Bucharest metropolitan area,
459 *Seismological Research Letters*, 76:574–580.
460 41. Roselli, I., V. Fioriti, I. Bellagamba, M. Mongelli, A. Tatì, M. Barbera, M. Magnani
461 Cianetti, and G. De Canio. 2017. Urban transport vibrations and cultural heritage sites in

462 Rome: the cases of the temple of Minerva amd the catacomb of Priscilla. *WIT Transactions*
463 *on Ecology and the Environment*, 223:335-343.
464 42. Shih C.Y., Y.G. Tsuei, R.J. Allemang, and D.L. Brown. 1988. Complex mode indication
465 function and its applications to spatial domain parameter estimation. *Mech. Syst. Signal*
466 *Process*, 2(4): 367-377.
467 43. Todorovska, M. 2009. Soil-Structure System Identification of Millikan Library North–South
468 Response during Four Earthquakes (1970–2002): What Caused the Observed Wandering of
469 the System Frequencies? *Bulletin of the Seismological Society of America*, 99(2A):626–635.
470 44. Trifunac, M.D. 1970. Wind and microtremor induced vibrations of a twenty-two story steel
471 frame building. *Sc. Rep. of Earthquake Engineering Research Laboratory of California*
472 *Institute of Techonology,* Pasadena, California, USA, pp. 52.
473 45. Ubertini, F., G. Comanducci, N. Cavalagli, A.L. Pisello, A.L. Materazzi, and F. Cotana.
474 2017. Environmental effects on natural frequencies of the San Pietro bell tower in Perugia,
475 Italy, and their removal for structural performance assessment. *Mechanical Systems and*
476 *Signal Processing.* 82(1):307-322.
477 46. Wyjadlowski, M. 2017. Methodology of dynamic monitoring of structures in the vicinity of
478 hydrotechnical works: Selected case studies. *Studia Geotechnica et Mechanica*, 39(4).
479

Figure 1. The historic centre of Lucca with the Clock Tower on the right.

Figure 2. The Clock Tower: view from Via Fillungo.

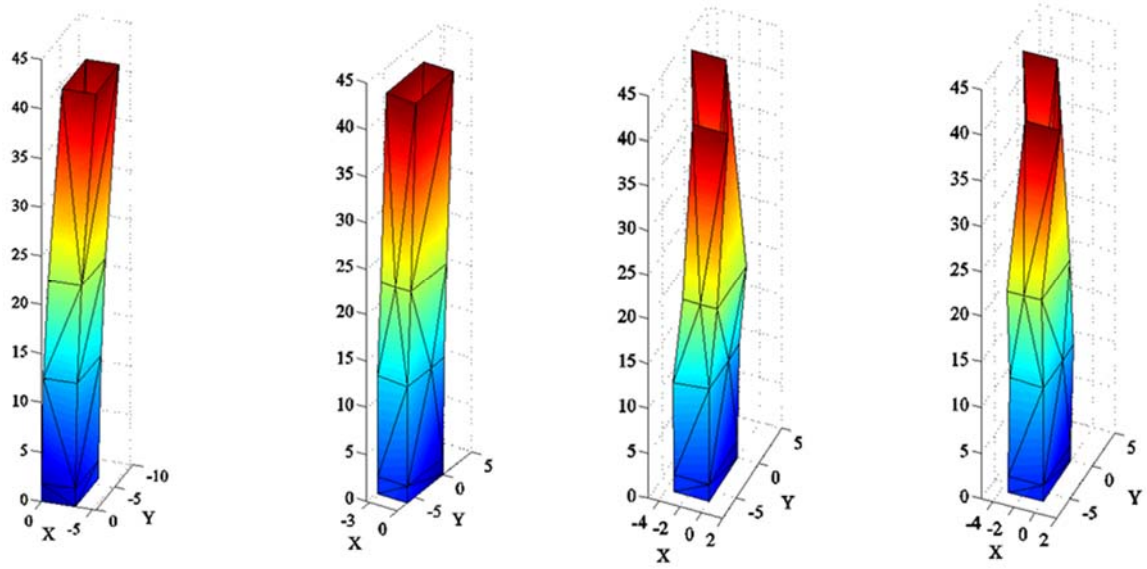

Figure 3. The tower's first four mode shapes.

Figure 4. Sensor S.943 at level +24 m inside the tower.

492

493 Figure 5. Sensor S.2 at level +37 m inside the tower.

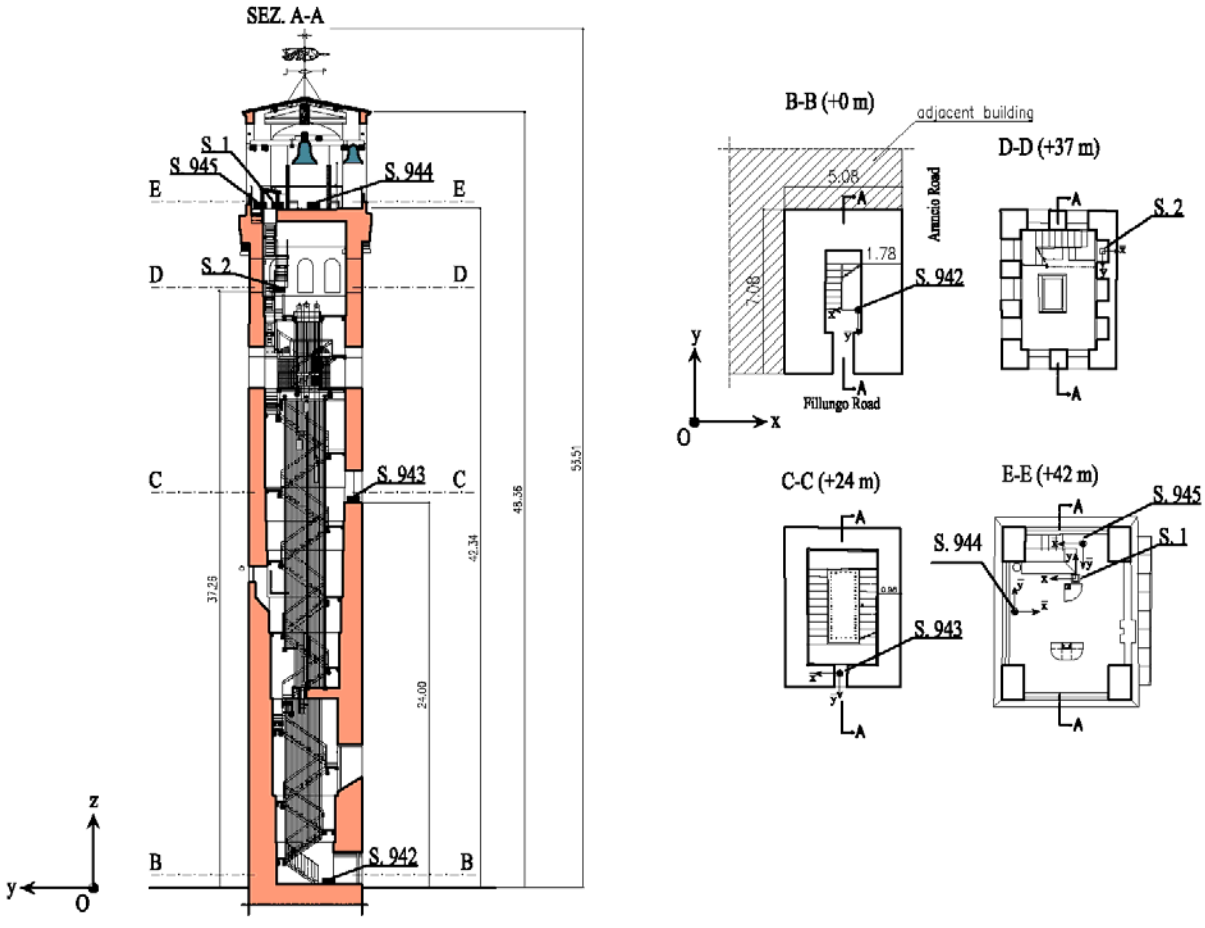

494

495 Figure 6. Sensor arrangement on the Clock Tower: sensors S.942, S.943, S.944, S.945 (SARA), sensors S.1, S.2 (AGI).

496

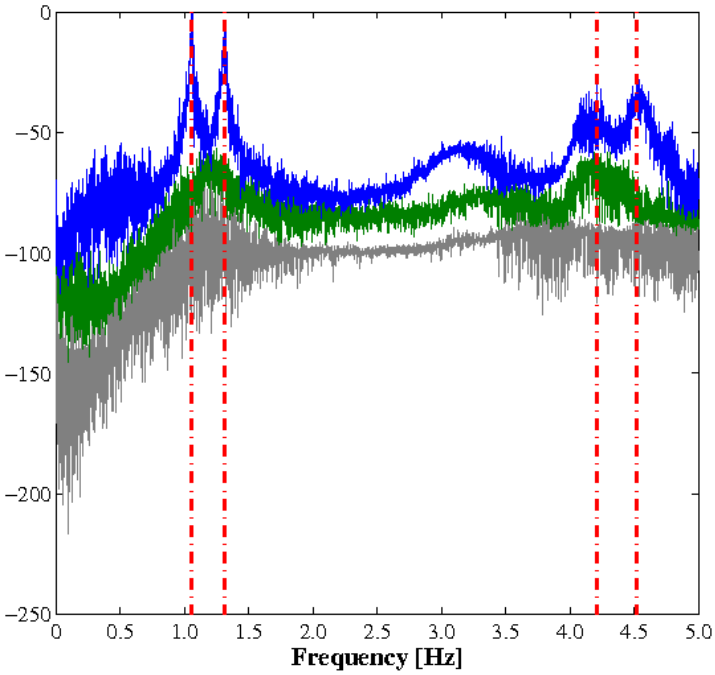

497

498 Figure 7. The three eigenvalues of the matrix $H[j\omega]^H H[j\omega]$ vs. the frequency on a log-magnitude scale.

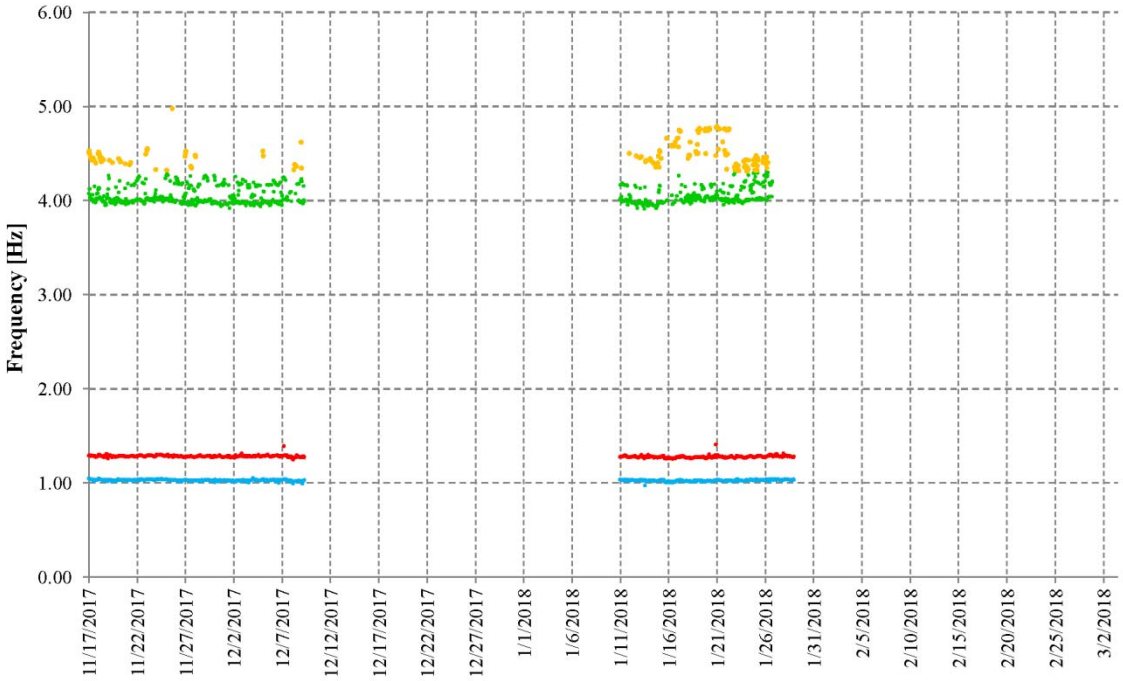

499

500 Figure 8. The tower's first four natural frequencies [Hz] detected by SS20 velocimeters during the monitoring period.

501

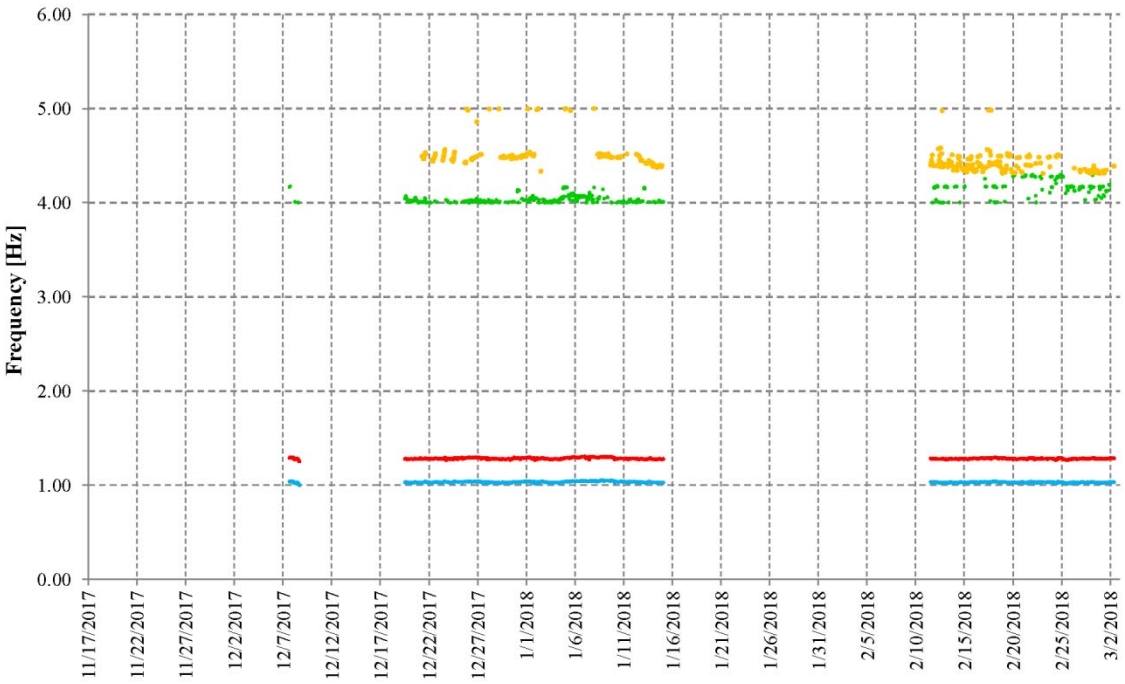

Figure 9. The tower's first four natural frequencies [Hz] detected by AGI accelerometers during the monitoring period.

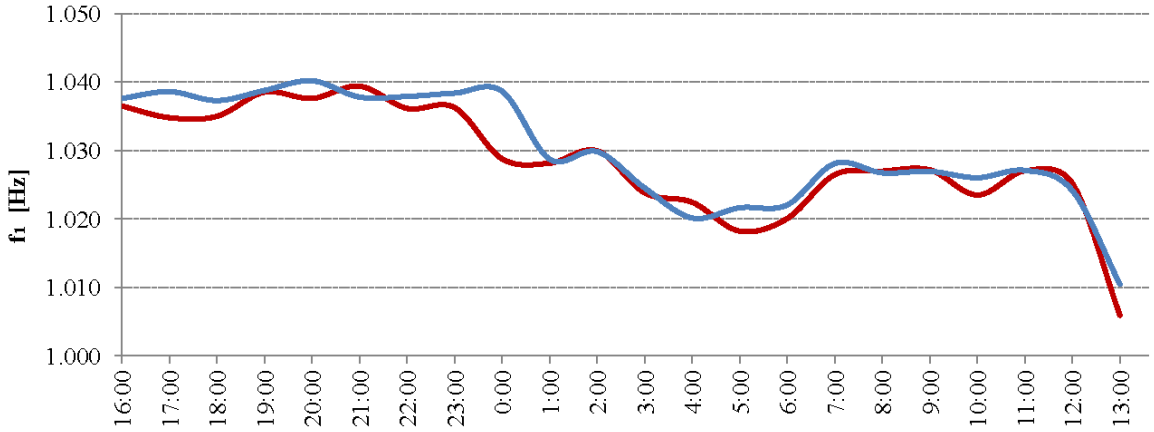

Figure 10. The tower's fundamental frequency obtained via AGI stations (blue) and SS20 stations (red) data from 7 to 8 December 2017 (respectively at 16:00 and 13:00).

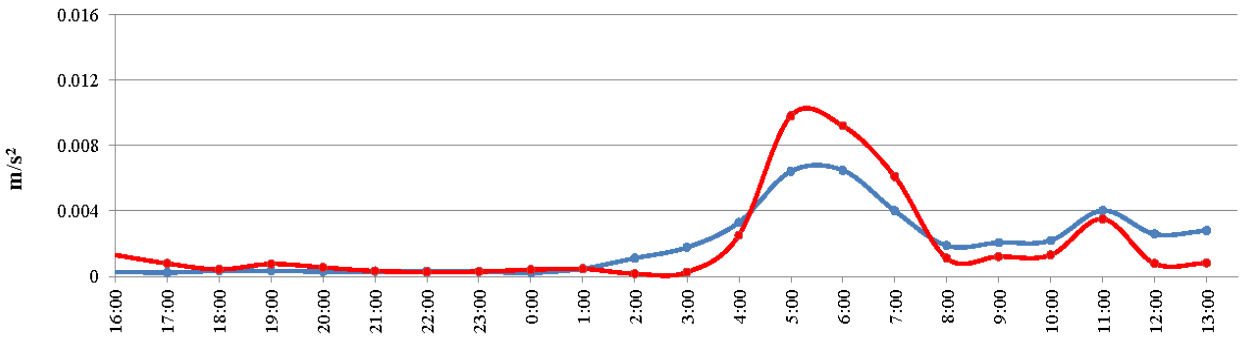

Figure 11. Maximum absolute accelerations along *x* recorded by the S.1 station (blue, +42 m) and the S. 945 station (red, +42 m) from 7 to 8 December 2017.

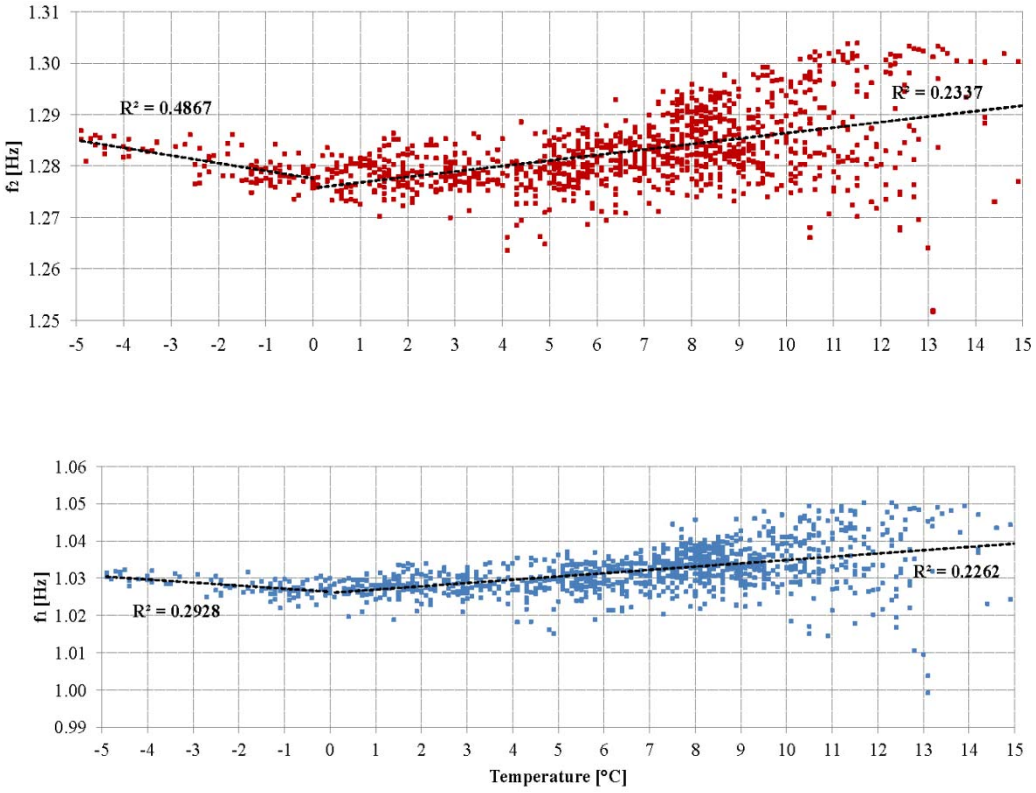

Figure 12. The first (blue) and second (red) natural frequencies of the tower [Hz] vs. temperature [°C].

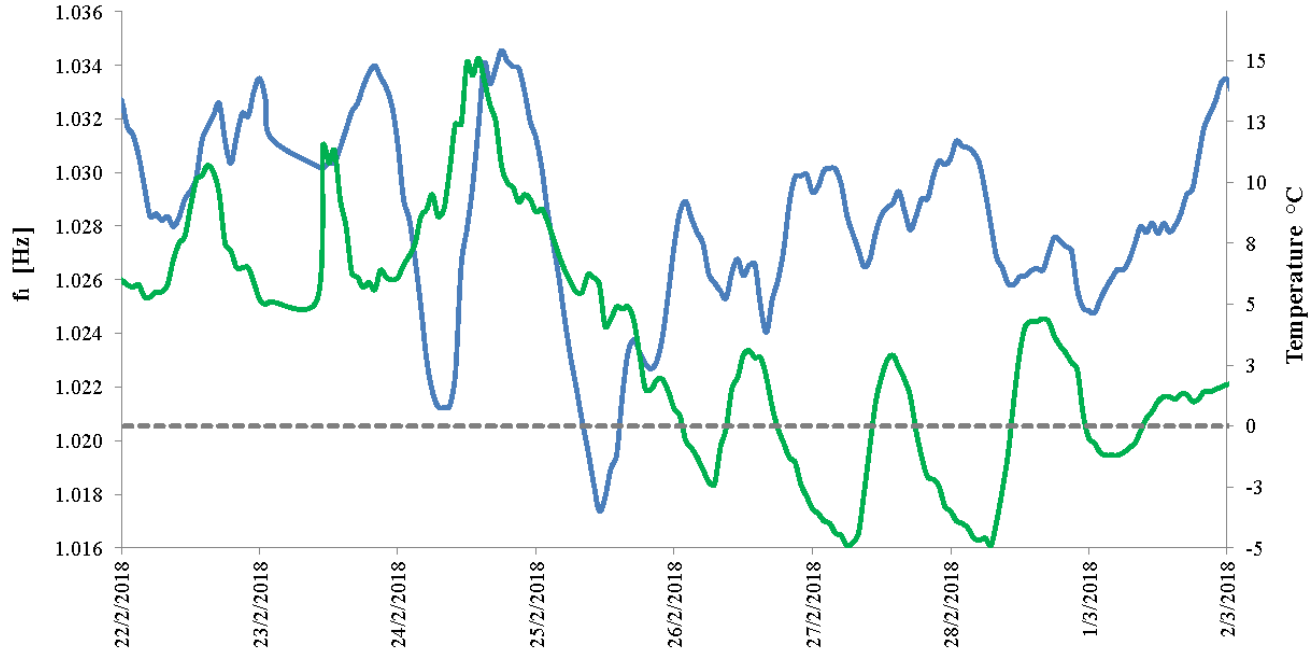

Figure 13. The tower's first (blue line) natural frequency [Hz] vs. temperature [°C] (green line), during February 2018.

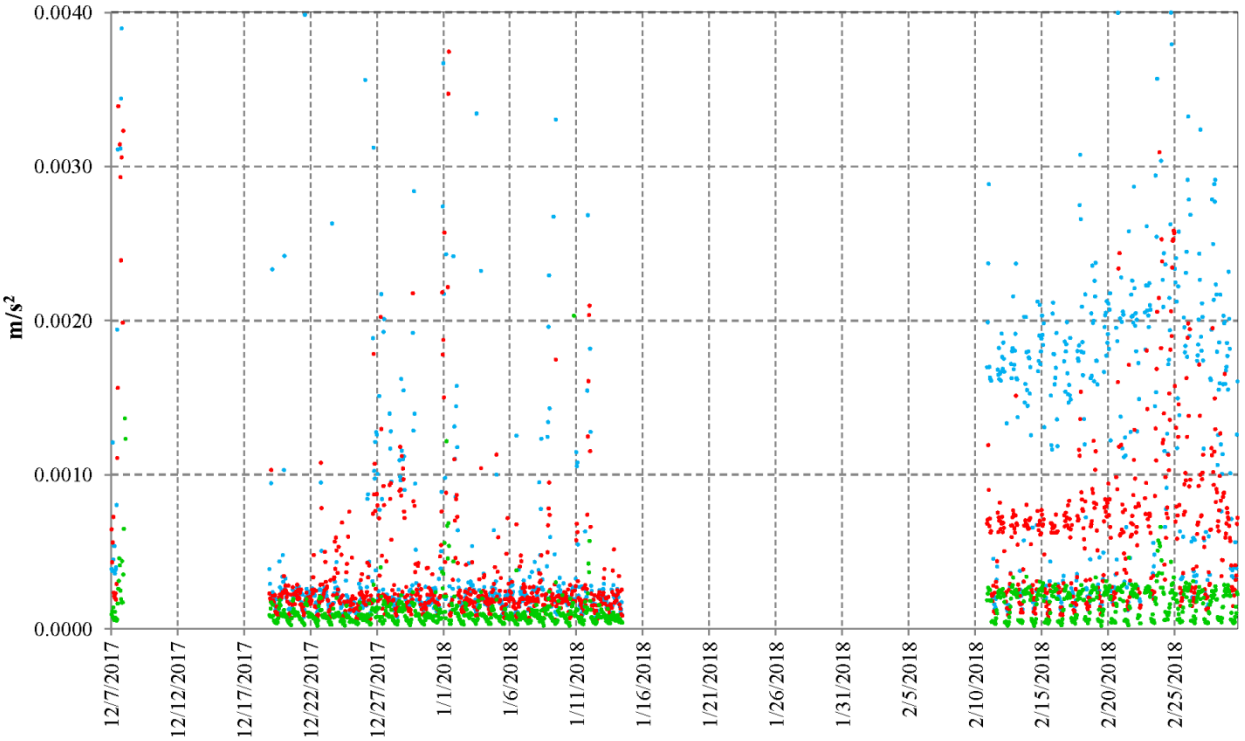

Figure 14. Maximum absolute values per hour of the accelerations recorded by AGI stations (S.2, +37 m) in the *x* (blue dots), *y* (red dots) and *z* (green dots) directions.

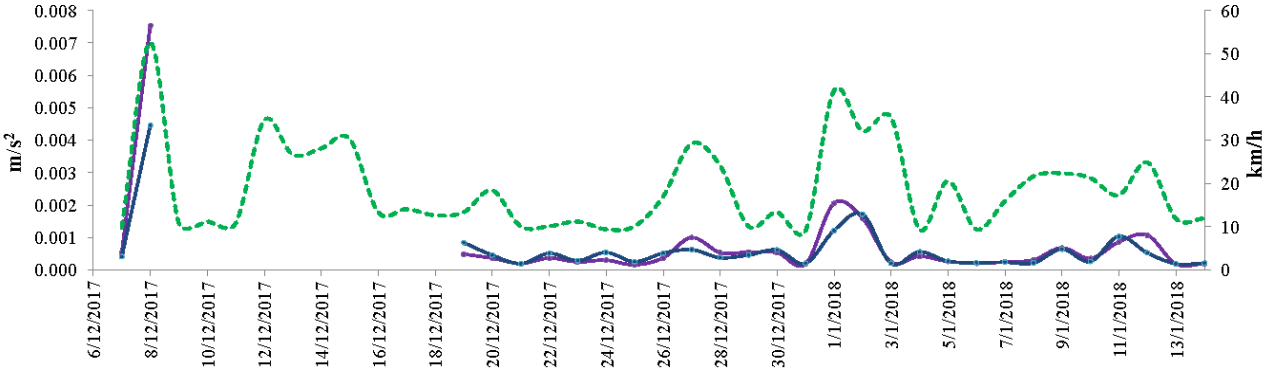

Figure 15. Daily average of the maximum hourly accelerations measured by S.2 vs. time along the *x* (blue) and *y* (red). directions. The dashed green line stands for the daily maximum wind speed. The correlation coefficients are R^2=0.5654 (daily average *x* – wind speed) and R^2=0.5018 (daily average *y* – wind speed).

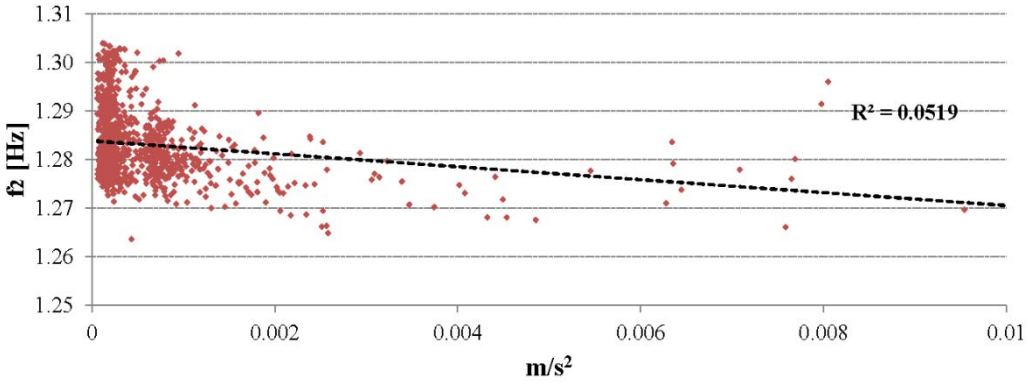

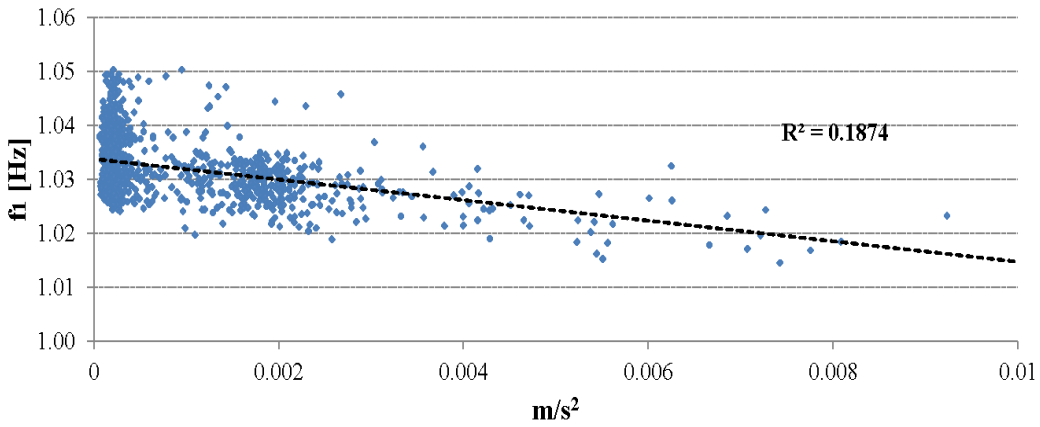

Figure 16. The first (blue) and second (red) natural frequencies of the tower [Hz] vs. the maximum acceleration experimented by the tower [m/s^2]

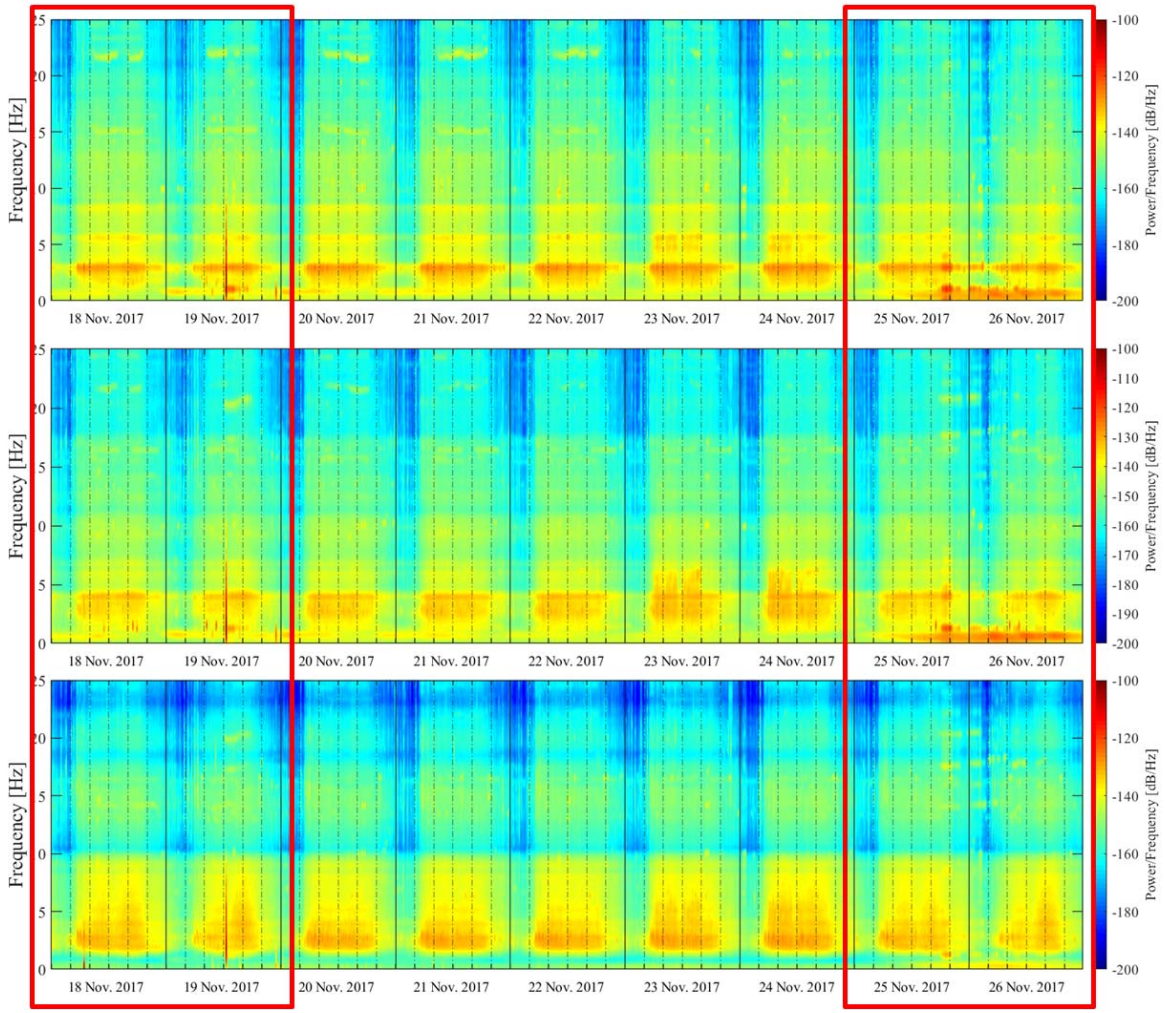

Figure 17. Spectrogram of the signal recorded by S.942 (+ 0,00 m) in the *x* (up), *y* and *z* (bottom) directions from 18 to 26 November 2017. Week-ends are highlighted by the red boxes.

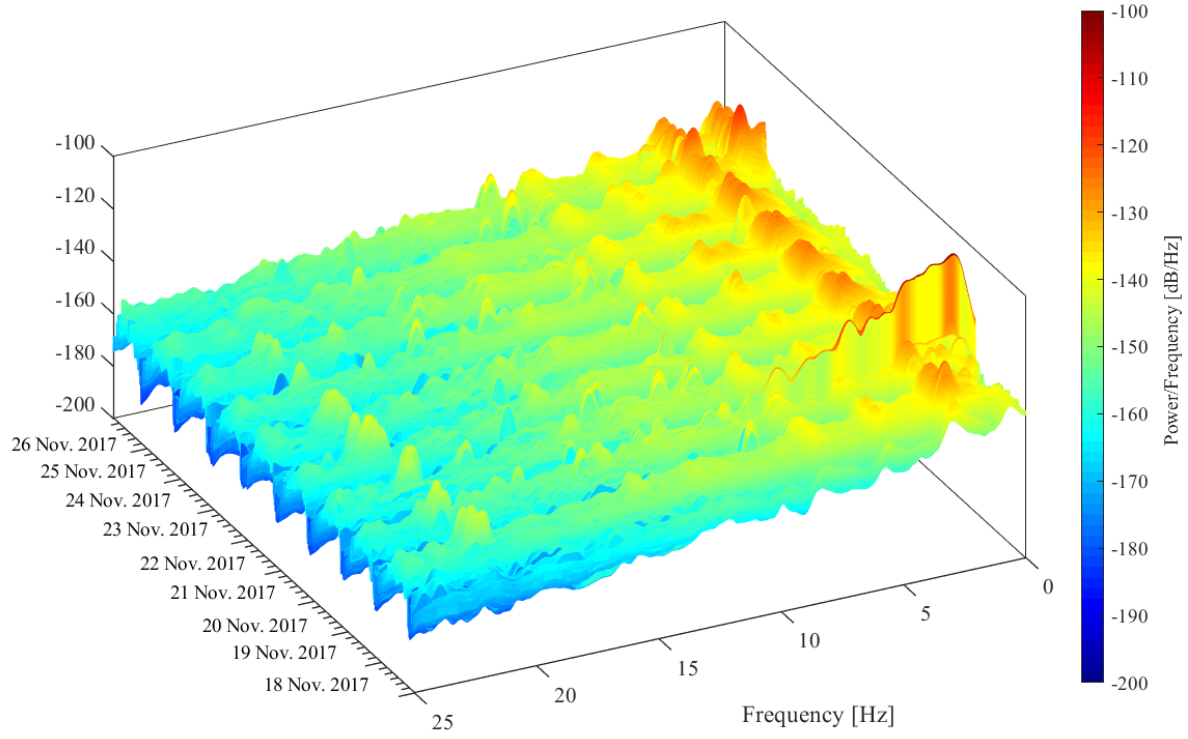

538

539 Figure 18. Three-dimensional spectrogram of the signal recorded by S.942 (+0,00 m) in the *x* direction from 18 to 26

540 November 2017.

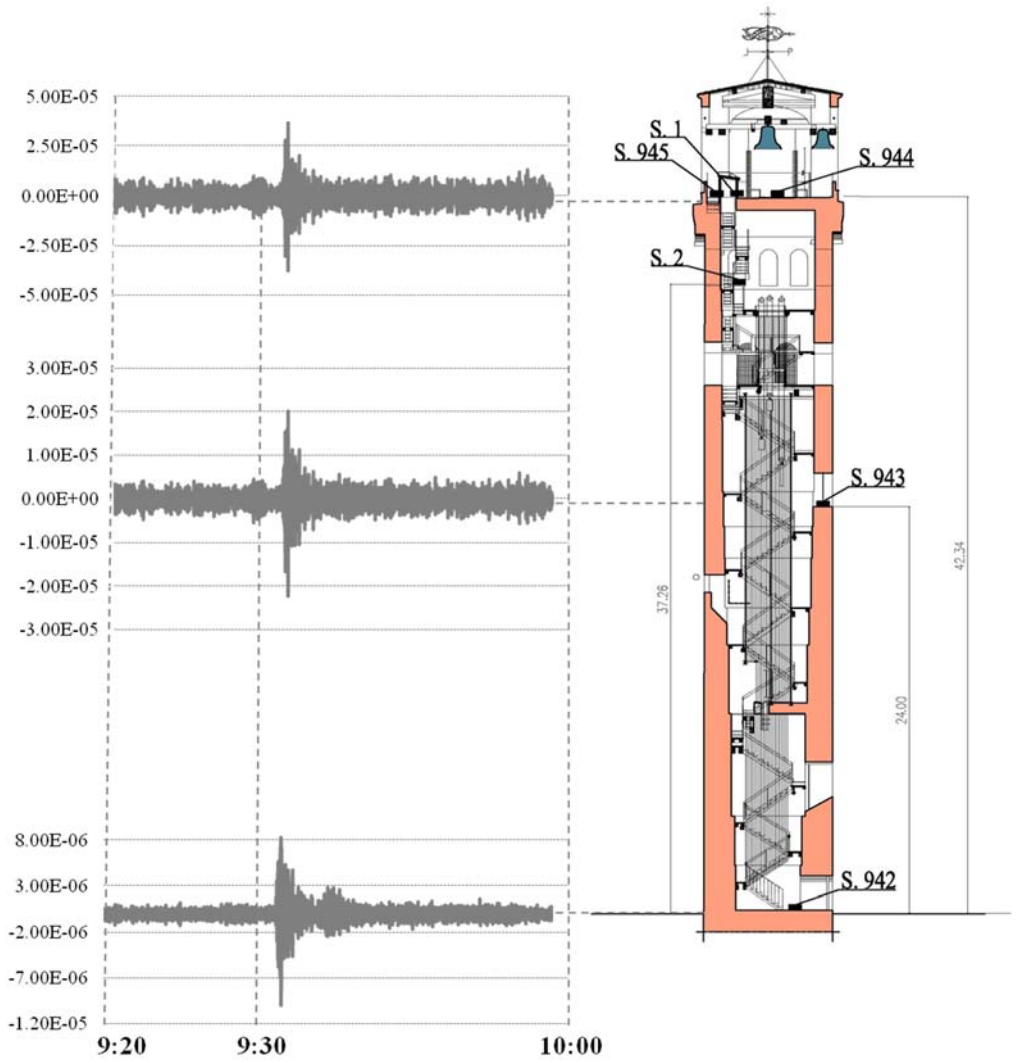

Figure 19. Signal of the Peru earthquake recorded on the tower in the *x* direction by S.942, S. 943, S.944 on 14 January 2018 from 9:33 (UTC) onward. Signal amplitude is in m/s^2.

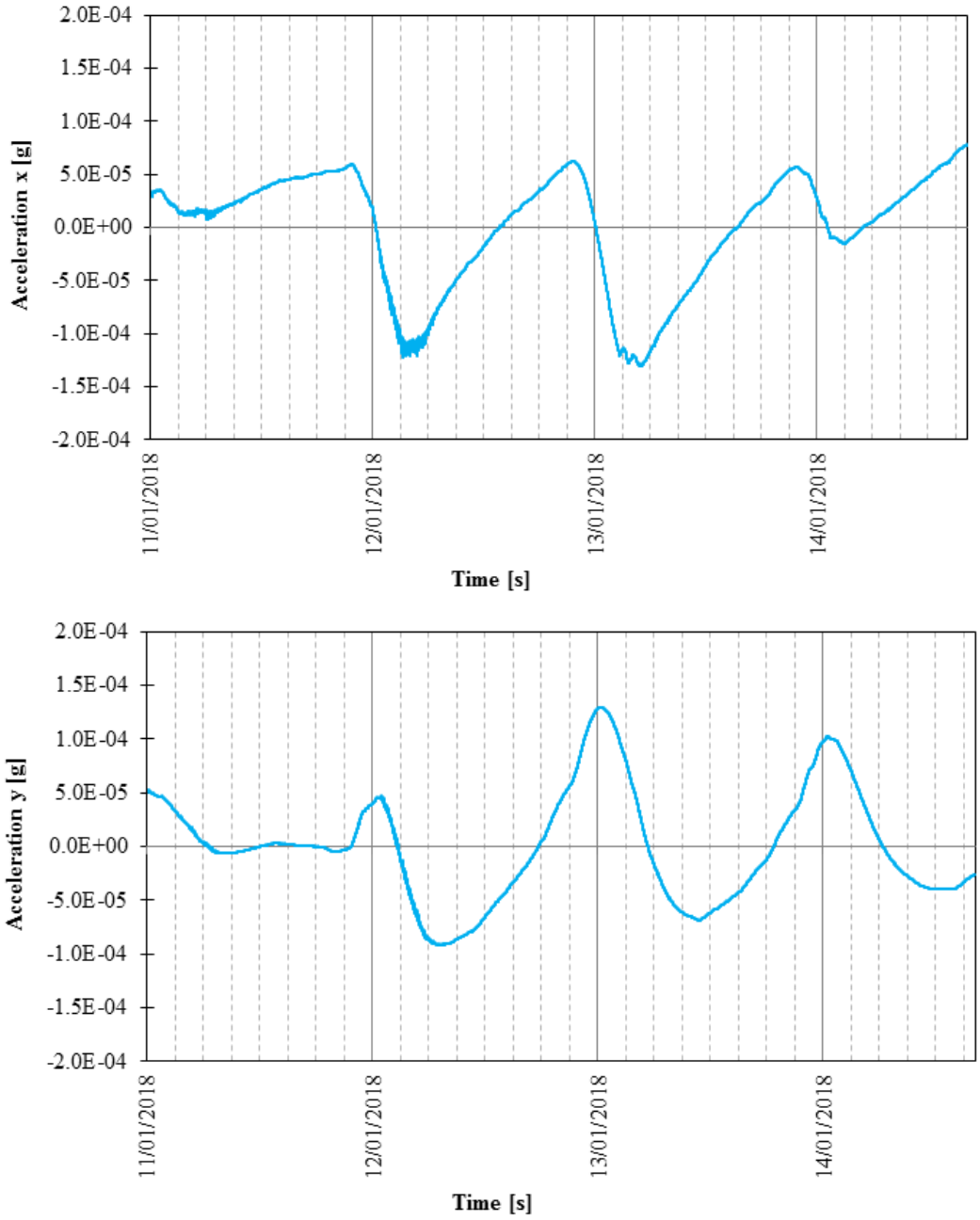

Figure 20. Low-pass filtered accelerations recorded by S.2 along the *x* and *y* (bottom) directions from 11 to 14 January 2018.

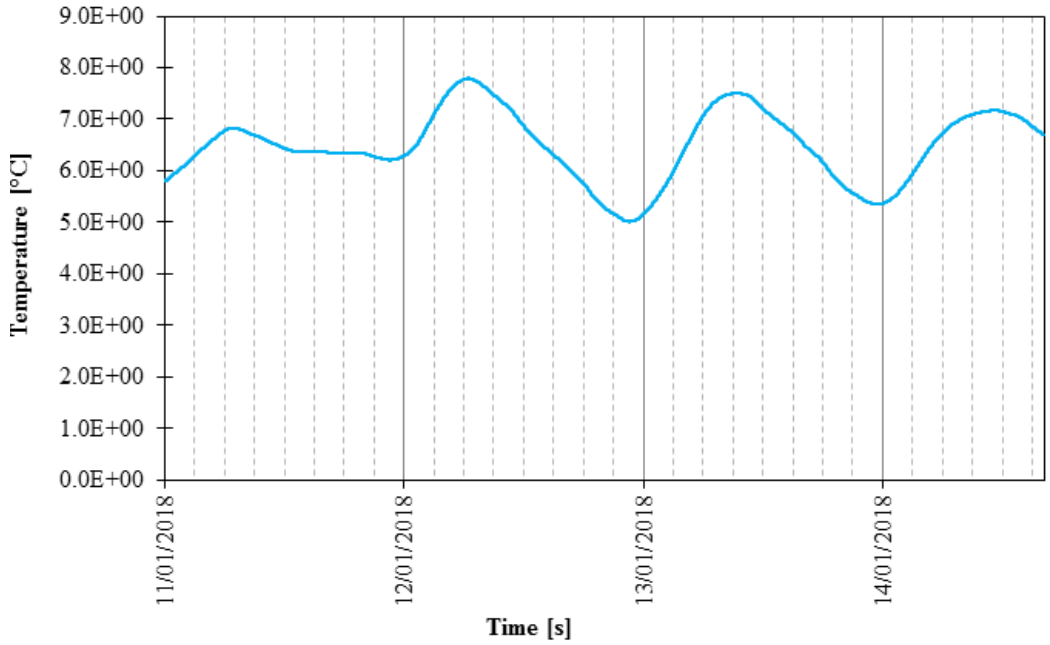

549

550 Figure 21. Temperatures recorded by the sensor installed inside S.2 from 11 to 14 January 2018.

551

Mode	Frequency [Hz]	Mode shape
1	1.05	Bending
2	1.30	Bending
3	4.20	Torsional
4	4.50	Torsional + bending

552 Table 1. Natural frequencies measured during the preliminary campaign on 25 November 2016 (Pellegrini et al. 2017).

553

	$\mathbf{f_1}$ [Hz]	$\mathbf{\Delta_1}$ [%]	$\mathbf{f_2}$ [Hz]	$\mathbf{\Delta_2}$ [%]	$\mathbf{f_3}$ [Hz]	$\mathbf{\Delta_3}$ [%]	$\mathbf{f_4}$ [Hz]	$\mathbf{\Delta_4}$ [%]
SS20	**1.0281**	3.65	**1.2813**	3.40	**4.0524**	8.67	**4.4858**	10.68
AGI	**1.0318**	2.94	**1.2829**	2.63	**4.0712**	7.26	**4.4654**	15.83

554 Table 2. Mean values $\mathbf{f_i}$ of the natural frequencies measured by the two instruments during the monitoring period and

555 their variation $\Delta_i = (f_i^{1} - f_i^{99})/ f_i^{1}$, where f_i^{1} and f_i^{99} represent the first and 99th percentile of the dataset, respectively.

556

	$\mathbf{\xi_1}$ [%]	$\mathbf{\Delta_1}$ [%]	$\mathbf{\xi_2}$ [%]	$\mathbf{\Delta_2}$ [%]	$\mathbf{\xi_3}$ [%]	$\mathbf{\Delta_3}$ [%]	$\mathbf{\xi_4}$ [%]	$\mathbf{\Delta_4}$ [%]
SS20	**0.90**	165	**1.26**	150	**2.03**	450	**1.88**	885
AGI	**0.69**	95	**0.85**	64	**1.41**	628	**1.01**	983

557 Table 3. Mean values $\mathbf{\xi_i}$ of the modal damping ratios measured by the two instruments during the monitoring period and

558 their variation $\Delta_i = (\xi_i^{5} - \xi_i^{95})/ \xi_i^{5}$, where ξ_i^{5} and ξ_i^{95} represent the fifth and 95th percentile of the dataset, respectively.

559

560

561

Date	Time (UTC)	Location	Magnitude
11/19/17	12:10:12	Parma	**3.3**
11/19/17	**12:37:44**	**Parma**	**4.4**
12/03/17	23:34:11	Amatrice	**4.0**

Table 4.Earthquakes recorded on the Clock tower in the monitoring period.

Date	Time (UTC)	Location	Magnitude
11/17/17	22:34:21	China	**6.4**
11/19/17	09:25:50	New Caledonia	**6.4**
11/19/17	15:09:04	New Caledonia	**6.6**
11/19/17	22:43:31	New Caledonia	**6.9**
11/30/17	06:32:50	Central Mid-Atlantic Ridge	**6.3**
12/01/17	02:32:48	Iran	**6.2**
01/11/18	18.26:24	Myanmar	**6.0**
01/14/18	**09:18.44**	**Peru**	**7.1**
01/23/18	09:31:43	United States (sea)	**7.6**
01/24/18	10:51:19	Japan	**6.4**
01/25/18	01:15:59	India	**6.0**
01/25/18	02:10:37	Russia	**6.3**

Table 5.Teleseismic earthquakes recorded on the Clock tower in the monitoring period.